Chapter 9

An Optimized Hybrid Fuzzy-Fuzzy Controller for PWM-driven Variable Speed Drives

Nordin Saad, Muawia A. Magzoub, Rosdiazli Ibrahim and Muhammad Irfan

Additional information is available at the end of the chapter

http://dx.doi.org/10.5772/61086

Abstract

This paper discusses the performance and the impact of disturbances onto a proposed hybrid fuzzy-fuzzy controller (HFFC) system to attain speed control of a variable speed induction motor (IM) drive. Notably, to design a scalar controller, the two features of field-oriented control (FOC), i.e., the frequency and current, are employed. Specifically, the features of fuzzy frequency and fuzzy current amplitude controls are exploited for the control of an induction motor in a closed-loop current amplitude input model; hence, with the combination of both controllers to form a hybrid controller. With respect to finding the rule base of a fuzzy controller, a genetic algorithm is employed to resolve the problem of an optimization that diminishes an objective function, i.e., the Integrated Absolute Error (IAE) criterion. Furthermore, the principle of HFFC, for the purpose of overcoming the shortcoming of the FOC technique is established during the acceleration-deceleration stages to regulate the speed of the rotor using the fuzzy frequency controller. On the other hand, during the steady-state stage, the fuzzy stator current magnitude controller is engaged. A simulation is conducted via MATLAB/Simulink to observe the performance of the controller. Thus, from a series of simulations and experimental tests, the controller shows to perform consistently well and possesses insensitive behavior towards the parameter deviations in the system, as well as robust to load and noise disturbances.

Keywords: Indirect field-oriented control (IFOC), hybrid fuzzy-fuzzy control (HFFC), hybrid fuzzy-PI control (HFPIC), disturbances, genetic algorithm (GA)

1. Introduction

During the last forty years, induction motors have been largely utilized in applications that use variable speeds. In the industry, the term workhorse is used to refer to an induction motor.

With the development in the field of silicon-rectifier devices, the variable speed induction motor drives techniques began to emerge in the late 1960s. At that time, the principal of speed control was only based on the steady state aspects of an induction machine. The rigorous research in this field has made possible the emergence of more techniques in industrial drives. One of the techniques that previously used for drives control is the V/f ratio that has been applied in an open-loop speed control of drives that normally need low dynamics. In addition, the slip frequency control technique is also effective for producing improved dynamics. Until the emergence of field-oriented controls (FOCs), this technique, based on all the high-performance induction motor (IM) drives, was considered as an industry standard for AC drives whose dynamics resemble DC motors [1–2, 19]. Hence, the invention of vector control and FOC are considered as the most significant factors in AC motor drives that boosted programs related to the development and research for improving control performance. Several benefits of process control can be obtained by adjusting the speed of the drive motors, such as varying speeds for its operation process, better control of speed variation, work efficiency, precise control for positioning, tension or torque, energy saving, and compensation of process varying variables [2].

Zadah, in 1965, described Fuzzy Logic as a novel kind of mathematical set approach consisting of a fuzzy set theory that is considered as a basic theory of the fuzzy logic. A fuzzy control system is established by applying a principle of fuzzy logic that consists of three phases: fuzzification, inference engine, and defuzzification. The inputs are converted into fuzzy sets in an initial phase. An inference engine defines the fuzzy rules in the next phase that links the outputs by using the sets of inputs via explicit rules. Finally, the conclusions are inferred by combining the outcomes of the fuzzy rules, which is then transformed into a sharp value from the fuzzy sets [3, 13].

In order to provide an effective means for a variable speed drive (VSD) control, several research studies exist that are based on control techniques and commercially available tools yielding a high degree of performance and reliability. Hence, a PLC-based hybrid-fuzzy control for pulse-width modulation PWM driven VSD is examined that depends upon the s-domain transfer function in a scientifically presented model of an original plant by keeping the V/f ratio at a constant value as in [5]. Notably in [5], the optimizations of the controller's performance against the parameter variations and external disturbances are not fully considered. Hence, the disadvantages of the FOC method and the results gained from the simulation are overcame by implementing two stage controllers as explain in [6–8], though all the practical implementations are quite satisfactory. Moreover, the satisfactory results are achieved by applying some controller algorithms for controlling the speed of an IM as in [9, 10].

Generally, by using simple solutions, fuzzy systems are capable of managing non-linear, complicated, and at times mathematically intangible dynamic systems [11]. Though, it is not an easy task to get an optimal set of fuzzy membership rules and functions, the designer needs to invest some times, skills, and experience for the tiresome fuzzy tuning exercise. Even though an iterative and heuristic process for transforming the membership functions to enhance performance has been recommended, in principle, there is no common method or rule for the fuzzy logic setup [11]. A lot of researchers have recently considered numerous intelligent schemes for the purpose of tuning the fuzzy system [12–17]. For instance, the genetic algorithm (GA) and neural network (NN) approach to optimize either the membership rules or functions

http://dx.doi.org/10.5772/61086

have turned into a trend in the development of the fuzzy logic system [11]. The benefits of the GA approach, apart from involving less cost, it is easy to implement the procedures and requires a single objective to be assessed [22]. Figure 1 presents the basic configuration of GA for a fuzzy control system with fuzzifier, defuzzifier, and an inference engine.

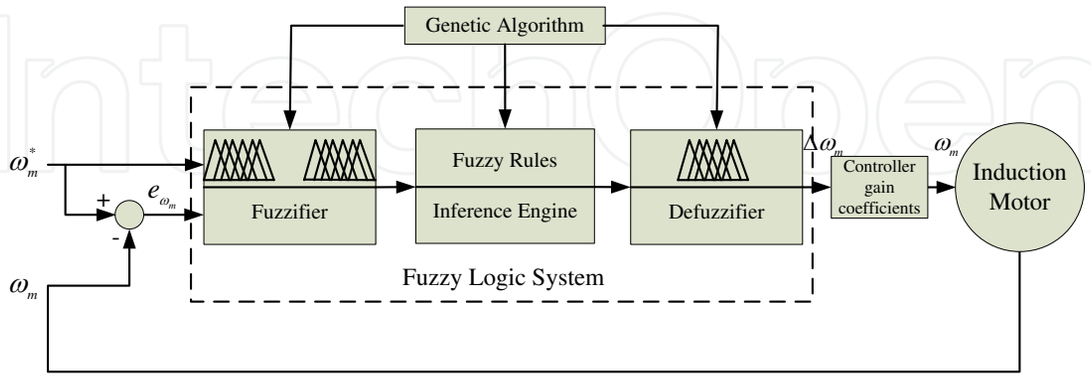

Figure 1. Genetic algorithm for a fuzzy control system.

A GA is employed in this research to attain the rules of the fuzzy inference system. However, the key aim of this study is to compare the performance of a fuzzy controller built on heuristics with a controller developed via the optimization technique.

Therefore, the best combination between the fuzzy input-output variables is needed to be discovered to enhance the inference rules of a fuzzy controller for a particular range of the fuzzy logic controller operation.

The FOC has two features [4, 6] that have been implemented in this work. Firstly, it is not able to do frequency control directly, due to the fact that the supply frequency changes during the period of acceleration-deceleration of the FOC while the slip frequency remains the same. Furthermore, in the presence of a torque command, the magnitude of a supply current magnitude remains stable.

The application of the FOC method has commonly been effective in achieving elevated performances in adjustable speed induction motor drives, however, it still suffers the following disadvantages [6]:

i. When evaluating certain integrals (i.e., the error accumulation), the degradation will be in the steady-state if the control time is extended and the outcome will be a transient responses owing to too much drift and accumulation of error in the values of the parameters;

ii. Susceptibility of the parameter deviations;

iii. There should be a steadiness in control and the calculation must be set off right from an initial state;

iv. Complex calculation is included in the final step.

The simulation and modeling of an induction motor controller constructed using MATLAB/ Simulink and the examination of the performance of the controllers (i.e., hybrid fuzzy-fuzzy controller (HFFC), hybrid fuzzy-PI controller (HFPIC), and indirect field-oriented controller (IFOC)) on the system are discussed in this paper. Also, in this study, the objective is to enhance the performance of the controller using HFFC. The purpose and context of this study are outlined in Figure 2.

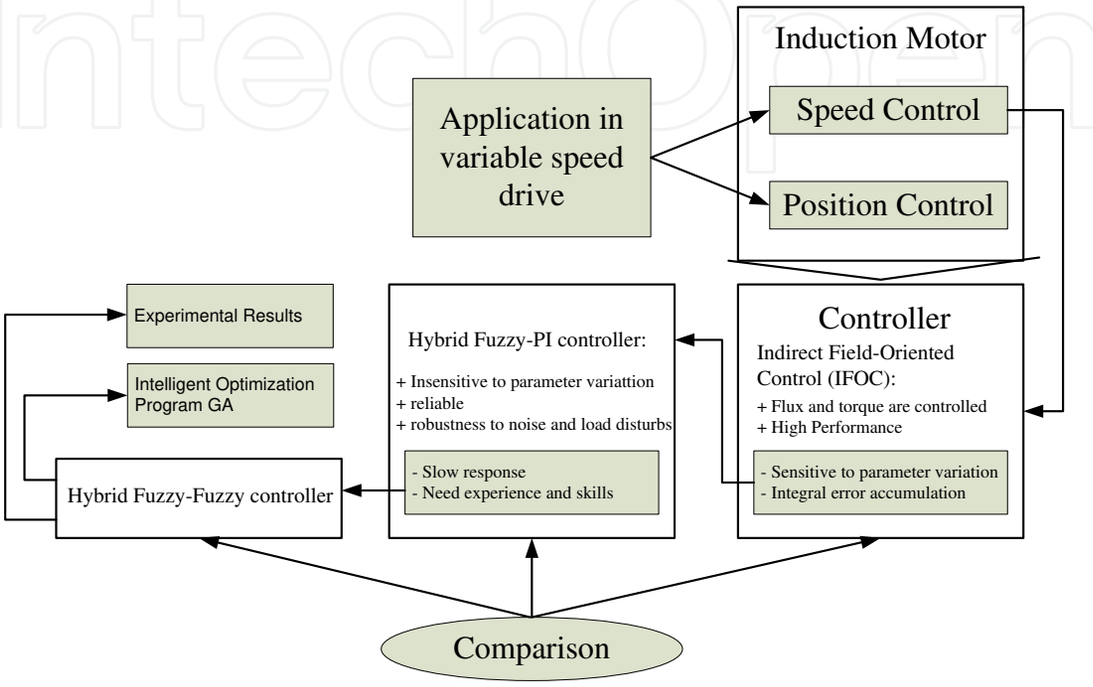

Figure 2. Overview of the study background.

The implementation of a fuzzy current amplitude controller on the induction motor model makes this work unique. This controller possesses the same supply features as FOC and insensitivity to the parameter variation for the motor and system robustness to noise and load disturbances are some of the advantages of this controller. Due to the fact that it provides better performance, the fuzzy current amplitude controller has been selected. While, the common structure of hybrid fuzzy-fuzzy controller is defined in Figure 3.

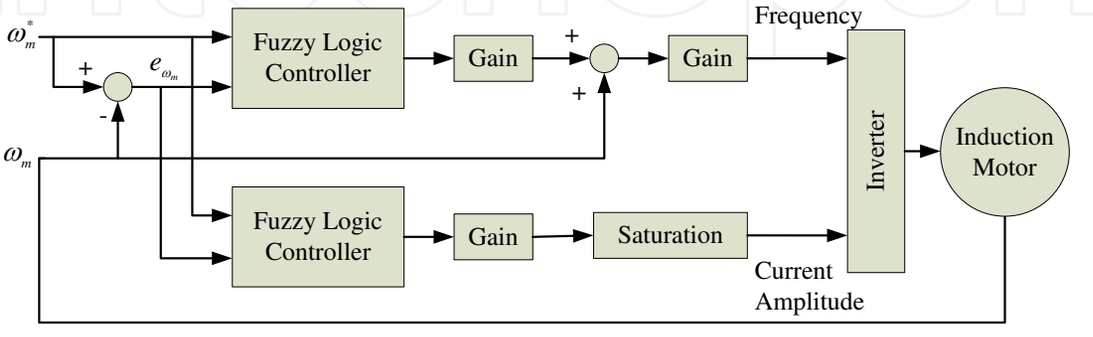

Figure 3. General structure of an HFFC.

http://dx.doi.org/10.5772/61086

2. Mathematical modeling

A higher order of mathematical equations that fall under one of the VSD control classifications can be used to model the dynamics of an induction motor. The steady-state model provides information about the performance of the induction motors in a steady state only. Table 1 provides the related parameters of IM. Figure 4 illustrates the IFOC model block of the proposed system for an IM.

Name	Symbol	Value
Resistance of stator	r_s	$29.4\times10^{-2}\ \Omega$
Resistance of rotor	r_r	$15.6\times10^{-2}\ \Omega$
Self-inductance of stator	L_s	$42.4\times10^{-3}\ H$
Self-inductance of rotor	L_r	$41.7\times10^{-3}\ H$
Magnetizing inductance	L_M	$41\times10^{-3}\ H$
Rotor inertia	J	$40.06\times10^{-2}\ Kg.m^2$
Damping constant	$B\ or\ f$	$0.062\ N.m.s/rad$
Number of pairs of poles	P	3

Table 1. Electrical and mechanical parameters of the IM.

By employing a two-phase motor in a quadrature and direct axis, the dynamic model of the induction motor is developed. The description of the notations is tabulated in Table 2. The state-space model of an induction motor in a stationary reference frame can be derived with the help of the voltage and flux linkage relations of an induction motor in the reference frame that is randomly selected [11, 12].

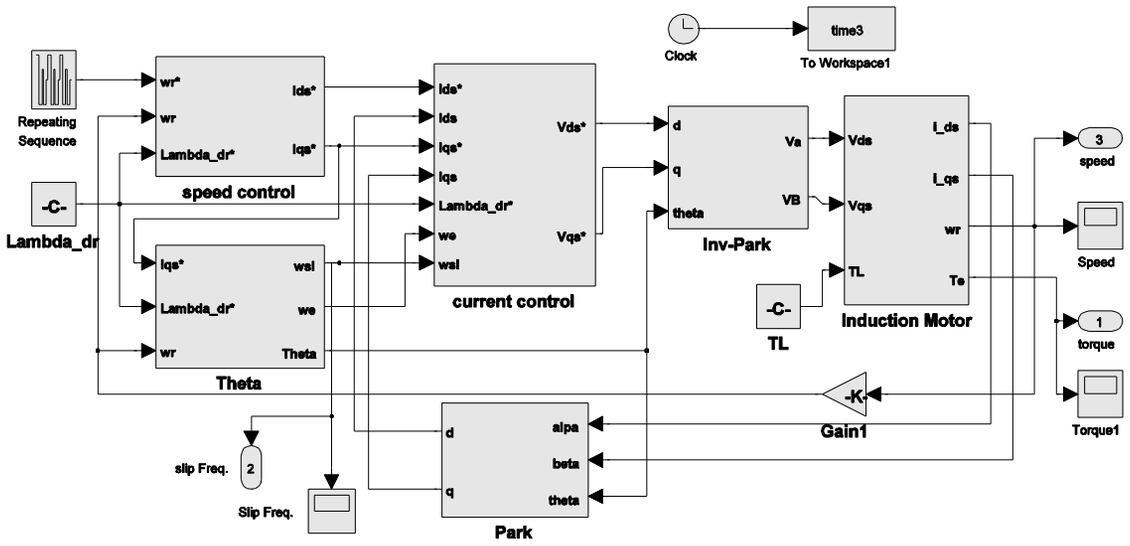

Figure 4. Proposed IFOC model block.

i_{ds}, i_{qs}	d- and q-axis stator current components, respectively, and expressed in stationary reference frame
i_{dr}, i_{qr}	d- and q-axis rotor current components, respectively, and expressed in stationary reference frame
L_M	Magnetizing inductance
L_s, L_r	Self-inductance of the stator and rotor, respectively
r_s, r_r	The resistance of a stator and rotor phase winding, respectively
T_e, T_l	Electromagnetic torque and Load torque reflected on the motor shaft, respectively
V_{ds}, V_{qs}	d- and q-axis stator voltage components, respectively, and expressed in stationary reference frame
L_{ls}, L_{lr}	Leakage resistance of the stator and rotor, respectively
λ_{ds}, λ_{qs}	d- and q-axis stator flux components, respectively, and expressed in stationary reference frame
λ_{dr}, λ_{qr}	d- and q-axis rotor flux components, respectively, and expressed in stationary reference frame
ω_m, ω_r	Mechanical and electrical angular rotor speed, respectively
ω	Synchronous speed or dominant frequency
P	Number of pairs of poles
ρ	Operator $^{d}/_{dt}$
J	The inertia of the rotor kgm^2 or Js^2
B	The damping constant that represents dissipation due to windage and friction
$\gamma=\left[\frac{L_M^2 r_r + L_r^2 r_s}{\sigma L_s L_r^2}\right]$, $\sigma=1-\left[\frac{L_M^2}{L_s L_r}\right]$, $\beta=\left[\frac{L_M}{\sigma L_s L_r}\right]$, $\beta_1=\left[\frac{1}{\sigma L_s}\right]$, $\alpha=\left[\frac{r_r}{L_r}\right]$	

Table 2. Nomenclatures.

The final state-space model of an induction motor with the controlled stator currents in a stationary frame can be written as shown in equations (1)–(6).

$$\frac{di_{ds}^s}{dt} = -\gamma i_{ds}^s + \beta\omega_r \lambda_{qr}^s + \beta\alpha\lambda_{dr}^s + \beta_1 V_{ds}^s \tag{1}$$

$$\frac{di_{qs}^s}{dt} = -\gamma i_{qs}^s - \beta\omega_r \lambda_{qr}^s + \beta\alpha\lambda_{qr}^s + \beta_1 V_{qs}^s \tag{2}$$

http://dx.doi.org/10.5772/61086

$$\frac{d\lambda_{dr}^{s}}{dt} = -\alpha\lambda_{dr}^{s} - \omega_r\lambda_{qr}^{s} + \alpha L_M i_{ds}^{s} \tag{3}$$

$$\frac{d\lambda_{qr}^{s}}{dt} = -\alpha\lambda_{qr}^{s} + \omega_r\lambda_{dr}^{s} + \alpha L_M i_{qs}^{s} \tag{4}$$

$$\frac{d\omega_m}{dt} = -\frac{B}{J}\omega_m + \frac{1}{J}\left(T_e - T_l\right),\ \omega_r = \frac{P}{2}\omega_m \tag{5}$$

$$T_e = \left(\frac{3}{2}\right)\left(\frac{P}{2}\right)\frac{L_M}{Lr}\left(i_{qs}^{s}\lambda_{dr}^{s} - i_{ds}^{s}\lambda_{qr}^{s}\right) \tag{6}$$

Notably, the two features of the FOC that have been used in this research study are shown in Eq. (1) to (6). The first aspect that shows the supply frequency changes with the speed of a rotor [6] is given in Eq. (7) and (8).

$$\omega = \omega_r + \frac{P}{2}\omega_m \tag{7}$$

where:

$$\omega_r = \frac{3r_r T_l^{*}}{P\lambda_{dr}^{e^{*}2}} \tag{8}$$

If T^{*} is maintained constant during acceleration, then ω_r is also constant. In Eq. (7), as ω_m changes during acceleration, then ω has to be varied, so that Eq. (7) satisfies the first FOC feature. The second feature can be proven by substituting the conditions $\lambda_{qr}=0$ and $\lambda_{dr}=constant$ in Eq. (3) [6, 21].

$$\left|i_s\right| = \frac{2}{3}\sqrt{i_{ds}^2 + i_{qs}^2} \tag{9}$$

where:

$$i_{ds} = \frac{\lambda_{dr}^{e}}{L_M} = constant \tag{10}$$

$$i_{qs} = \frac{3L_r T^*}{PL_M \lambda_{dr}^{e*}} \tag{11}$$

Eq. (9) will be a constant if the torque command T^* is a constant, which satisfies the second feature. The Figure 5 shows that the speed response may be divided into two stages. For the HFFC, Table 3 shows the relationship between the inputs and outputs.

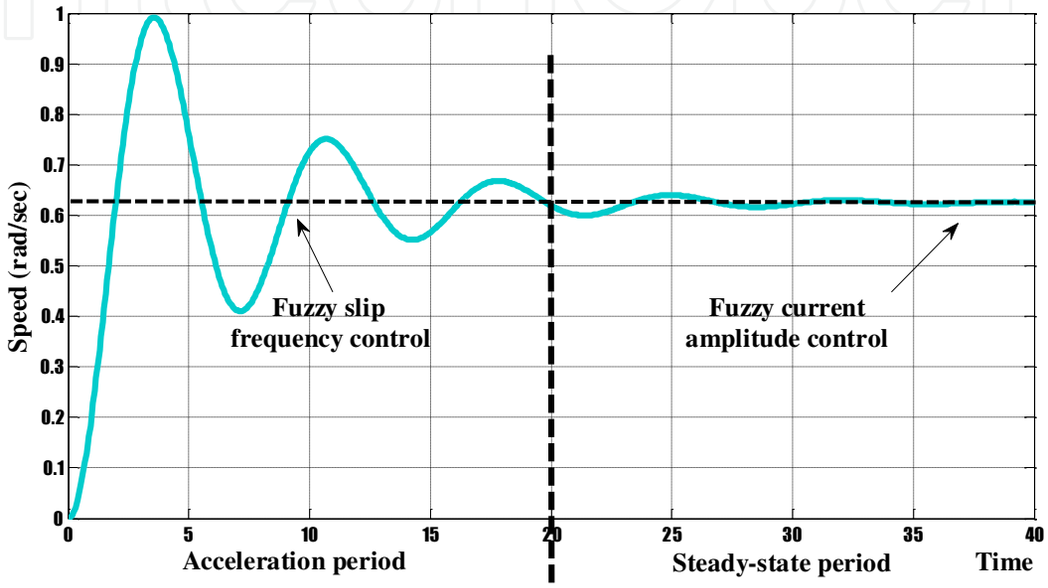

Figure 5. Speed response stages.

3. Design of the controllers

3.1. Fuzzy current amplitude controller

In the stage of acceleration-deceleration, the stator current magnitude is regulated as the system is driven by the maximum permissible values of an inverter. During the final steady-state period, the speed of the rotor is controlled by adjusting the magnitude of the stator current, while the supply frequency is kept constant. In the presence of a constant supply frequency, the relationship between torque-current may be expressed as follows [21].

$$T = \left[\frac{3P}{2}\right]\left[\frac{r_r L_M^2 i_s^2 \left[\omega - \frac{P}{2}\omega_m\right]}{r_r^2 + \left[L_M + L_{lr}\right]^2 \left[\omega - \frac{P}{2}\omega_m\right]}\right] \tag{12}$$

http://dx.doi.org/10.5772/61086

The values for the current amplitude are depicted as follows:

$$\left|i_s\right| = \begin{cases} 50.54 \ \left|i_s\right| \geq 50.54A \quad when\ \Delta\omega_m \neq 0 \\ \left|i_s\right| \ \ \left|i_s\right| < 50.54A \quad when\ \Delta\omega_m = 0 \end{cases} \tag{13}$$

The main phase from every input-output data couples is to create a fuzzy rule to find out a degree of every data-value in each affiliated area of its corresponding fuzzy domain. Consequently, a variable is assigned to a region having a maximum value.

	Supply Frequency	Current Amplitude	Rotor Speed	Control Objective
Acceleration	Change	Constant	Change	Speed Change
Steady-State	Constant	Change	Constant	Reduce Oscillation

Table 3. HFFC relationship.

A truth or rule degree is assigned to a newly generated fresh rule from the input-output data couples. Therefore, a rule degree can be defined as an extension of assurance to relate the current- and voltage-related functions with an angle. Usually, a degree that is a creation of the membership function degree of every variable in its corresponding area is assigned in a formulated technique.

A compatible fuzzy rule is created by each training data set that is placed in the fuzzy rule base. Consequently, each input-output data couples is preserved and the rules are generated. A two-dimensional form that can be explored by the fuzzy reasoning tool is used to tabulate a knowledge base or fuzzy rule.

Figure 6 demonstrates the general structure of the fuzzy logic control (FLC), a combination of knowledge base, fuzzification, a defuzzification, and inference engine.

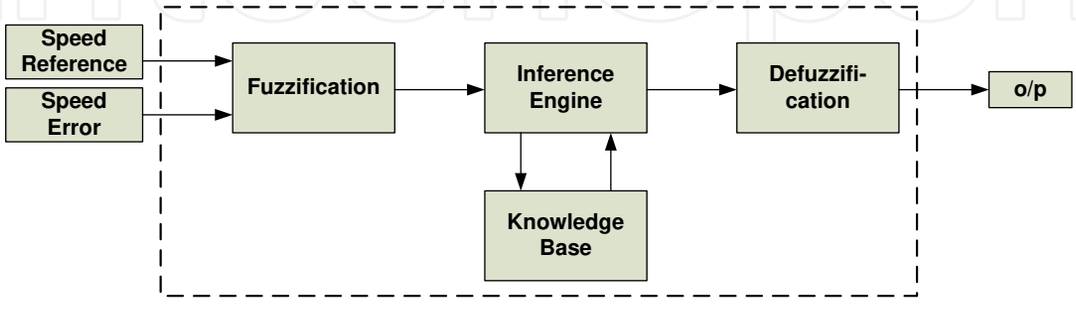

Figure 6. A general block diagram of FLC.

A speed error can be computed by comparing the reference speed and the speed signal feedback. The fuzzy knowledge base consists of membership functions of the inputs of the fuzzy controller including speed reference, error changing, and current amplitude/slip frequency outputs.

Stages	ω_m^*	A	f_A
Deceleration	-	-50.54	**NBB**
Steady-State	-120	-15.07	**NB**
-	-80	-12.79	**NM**
-	-40	-11.214	**NS**
-	0	0	**Z**
-	40	11.214	**PS**
-	80	12.79	**PM**
-	120	15.07	**PB**
Acceleration	-	50.54	**PBB**

Table 4. Speed, current amplitude, and fuzzy linguistic values.

3.2. Membership functions

Primarily, the fuzzy logic controller is used to convert the change of error variables and the crisp error into fuzzy variables, which is then plotted into the linguistic tags. All the membership functions and labels are connected with each other (Figures 7, 8, and 9), which comprises of two inputs and one output. The nine sets are formed by classifying the fuzzy sets that are outlined as follows:

Z: Zero	**PS**: Positive Small	**PM**: Positive Medium
PB: Positive Big	**NS**: Negative Small	**NM**: Negative Medium
NB: Negative Big	**PBB**: Positive Big Big	**NBB**: Negative Big Big

Table 5. Classification of the fuzzy sets

The previously defined seven numbers of linguistics, along with both inputs and outputs, include membership functions. Eq. (9) shows the samples of current amplitude of the two stages as shown in Table 4.

http://dx.doi.org/10.5772/61086

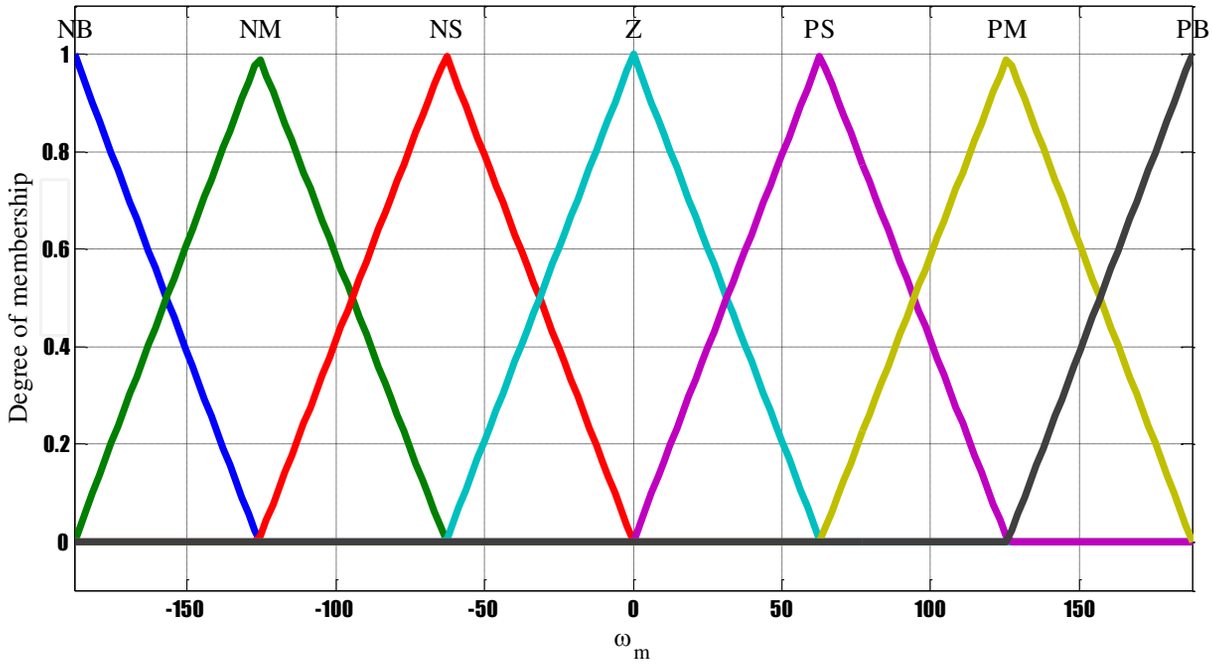

Figure 7. Membership function of speed reference.

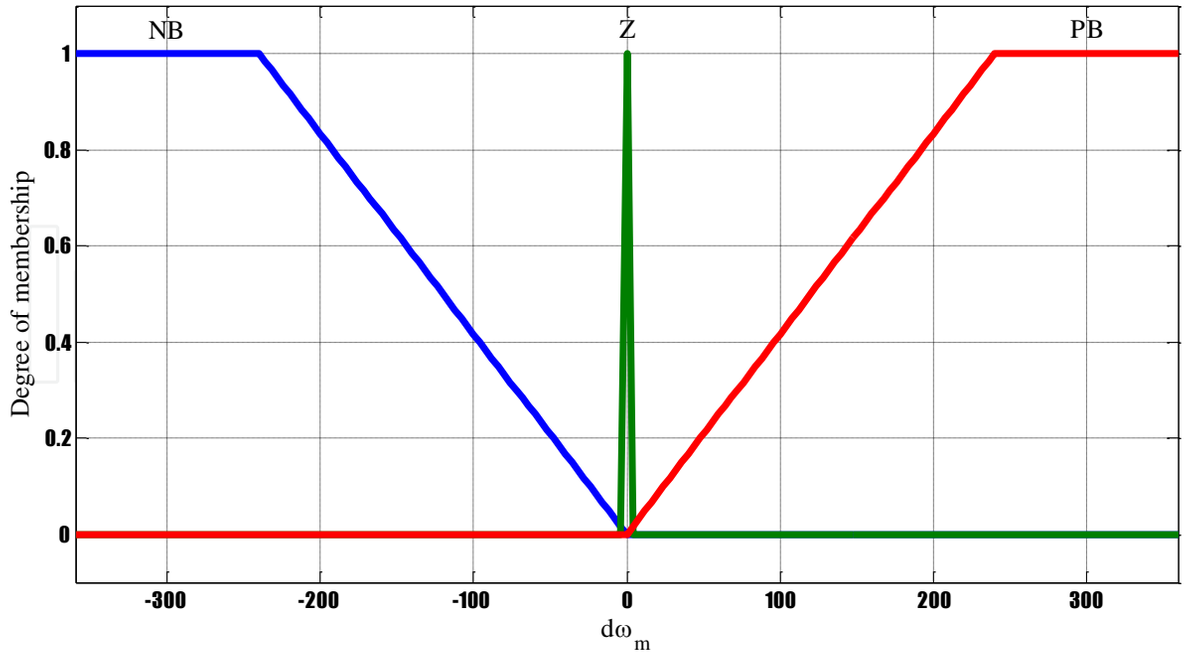

Figure 8. Membership function of speed error.

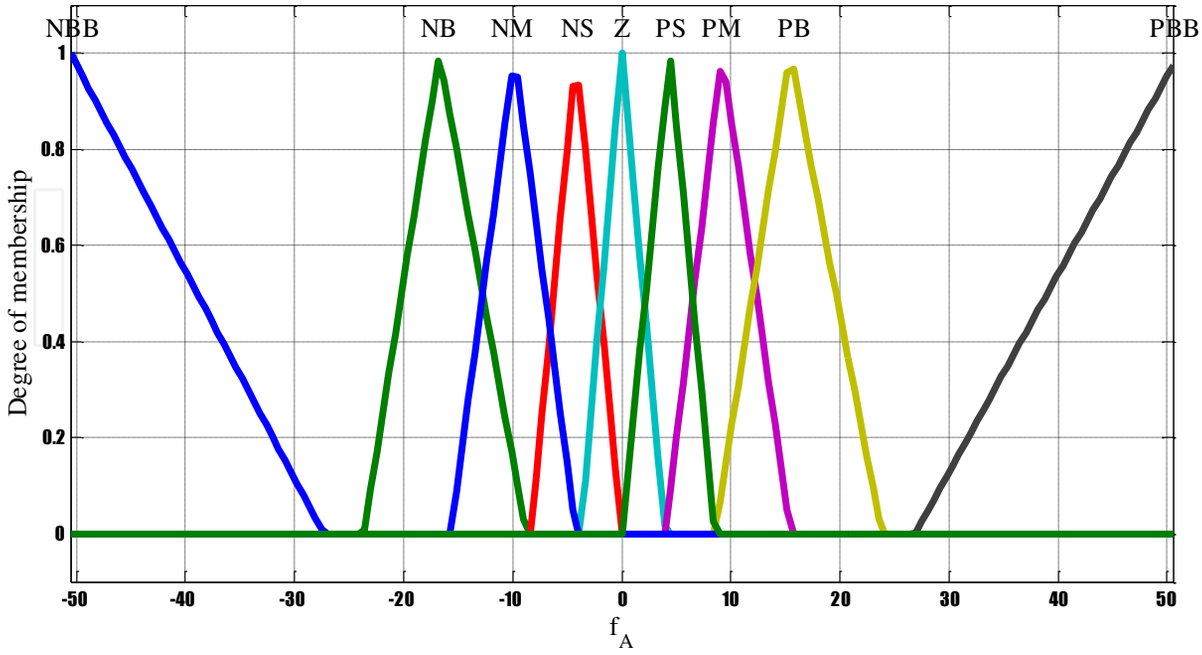

Figure 9. Membership functions of current amplitude.

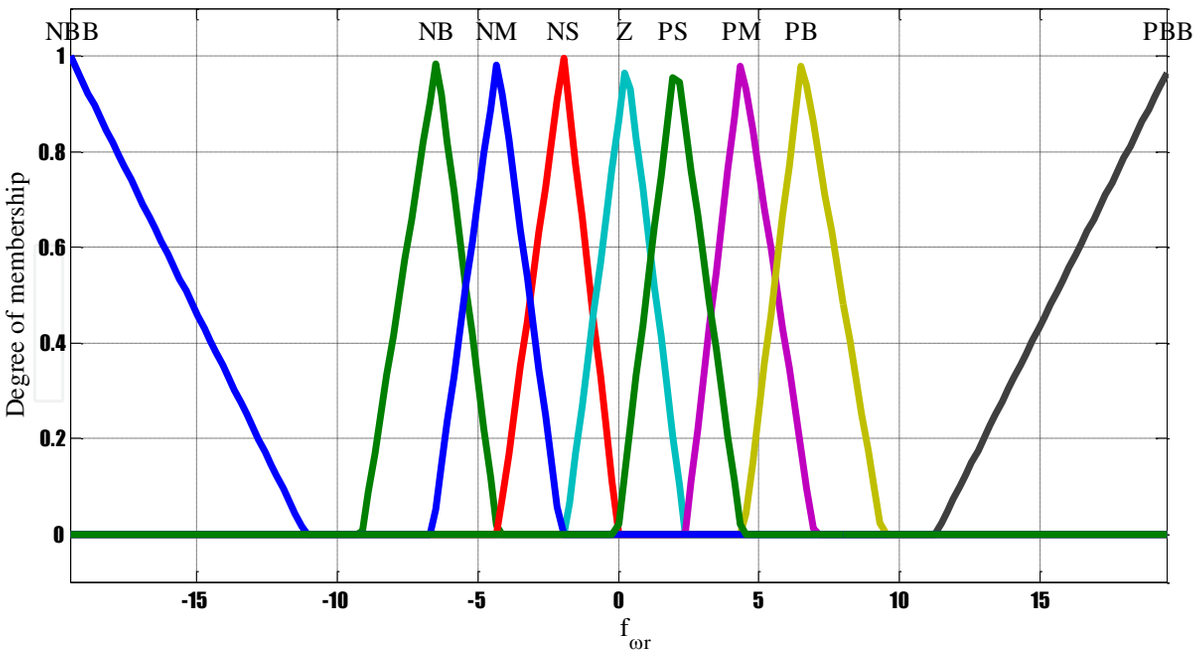

Figure 10. Membership functions of slip frequency.

http://dx.doi.org/10.5772/61086

3.3. Rule base

The fuzzy inputs can be plotted easily into the required output with the help of a useful tool, the rule base, as shown in Table 6.

Speed Error	Speed Reference						
	NB	**NM**	**NS**	**Z**	**PS**	**PM**	**PB**
NB	NBB	NBB	NBB	NBB	NBB	NBB	NBB
Z	NB	NM	NS	Z	PS	PM	PB
PB	PBB	PBB	PBB	PBB	PBB	PBB	PBB

Table 6. Rule matrix for fuzzy amplitude/slip controller.

3.4. Fuzzy frequency controller

A fuzzy frequency control is presented by using a frequency aspect of the field orientation principle. At a steady state phase, the torque command is a smaller value, whereas, the torque command becomes a larger value during the stage of acceleration-deceleration. The speed reference and rotor speed represent these values [4, 6, 11]. The following relations show a slip frequency at a steady-state.

$$\omega_r = \begin{cases} \dfrac{3r_r}{P\lambda_{dr}^{e^*2}} T_{acc} \;\; when\ \Delta\omega_m \neq 0 \\ \dfrac{3r_r}{P\lambda_{dr}^{e^*2}} \mu\omega_m \;\; when\ \Delta\omega_m = 0 \end{cases} \tag{14}$$

So the slip frequency can be written as:

$$\omega_r = f\left(\omega_m, \Delta\omega_m\right) \tag{15}$$

Eq. (14) shows the reference and speed error from the inputs of the fuzzy slip control. The membership functions of the output and input are depicted in Figures 7, 8, and 10. In addition, Table 6 shows the rule matrix. The samples of the slip frequency of the two stages can be obtained by Eq. (14), which is shown in Table 7.

3.5. Defuzzification

The fuzzy control action is executed with the help of simulating the human decision process via the interference engine, from the understanding of the linguistic variable expressions and

Stages	ω_m^*	ω_r	f_{ω_r}
Deceleration	-	-16.80	**NBB**
Steady-State	-120	-3.6328	**NB**
-	-80	-2.42192	**NM**
-	-40	-1.21096	**NS**
-	0	0	**Z**
-	40	1.21096	**PS**
-	80	2.42192	**PM**
-	120	3.6328	**PB**
Acceleration	-	16.80	**PBB**

Table 7. Speed, slip frequency, and fuzzy linguistic values.

the control rules. As a result, the knowledge base along with the inference engine is interconnected during the course of the control process. At first, through substituting the fuzzified inputs into rule base, the active rules are differentiated. Then, by employing one of the fuzzy reasoning methods, these rules are combined. The utmost distinctive fuzzy reasoning methods are the Max-Product and Min–Max. Since the Min-Max interference scheme is commonly used, it is also applied in this research. The fuzzy control actions are then regenerated with the help of defuzzification, which is deduced from the inference engine to a non-fuzzy control action. Thus, using the center of gravity method, the defuzzification is accomplished in the set of Eq. (16) to create a non-fuzzy control signal:

$$y = \frac{\sum_{i=1}^{n} u(i)\mu_{A,\omega_r}(y_i)}{\sum_{i=1}^{n} \mu_{A,\omega_r}(y_i)} \tag{16}$$

where, μ_{A,ω_r} is the degree of membership function.

[NBB=1, NB=2, NM=3, NS=4, Z=5, PS=6, PM=7, PB=8, PBB=9]

Whereas, the linguistic standards of the antecedents relate to the entire values as follows:

[NB=1, NM=2, NS=3, Z=4, PS=5, PM=6, PB=7]

However, it is essential to recognize the values of the precedents, fuzzy operators in the rule base weights, and fuzzy rules to form the rule base of a fuzzy controller; in this situation, the antecedents 1 and 2 and the other stated values are positioned in a matrix inside the MATLAB functions, as can be seen in the matrix below [24]:

http://dx.doi.org/10.5772/61086

$$\begin{bmatrix} Ant_1 Ant_2 Con_1 RwRC & \cdots & Ant_7 Ant_7 Con_7 RwRC \\ \vdots & \ddots & \vdots \\ Ant_3 Ant_3 Con_3 RwRC & \cdots & Ant_{21} Ant_{21} Con_{21} RwRC \end{bmatrix}$$

Where, Ant_n: antecedent n, Ant_n: antecedent n, Con_n: consequent n, Rw: rule weight, and RC: rule connection. Finally, the input/output variables range and the membership function data are in the same MATLAB function. The MATLAB FIS (Fuzzy Inference System) file is the output of this function that relates to a structure in which all the information of fuzzy inference of the system is incorporated, which is utilized as a fuzzy controller in the feedback scheme of the Simulink library. The flowchart procedure is shown in Figure 11.

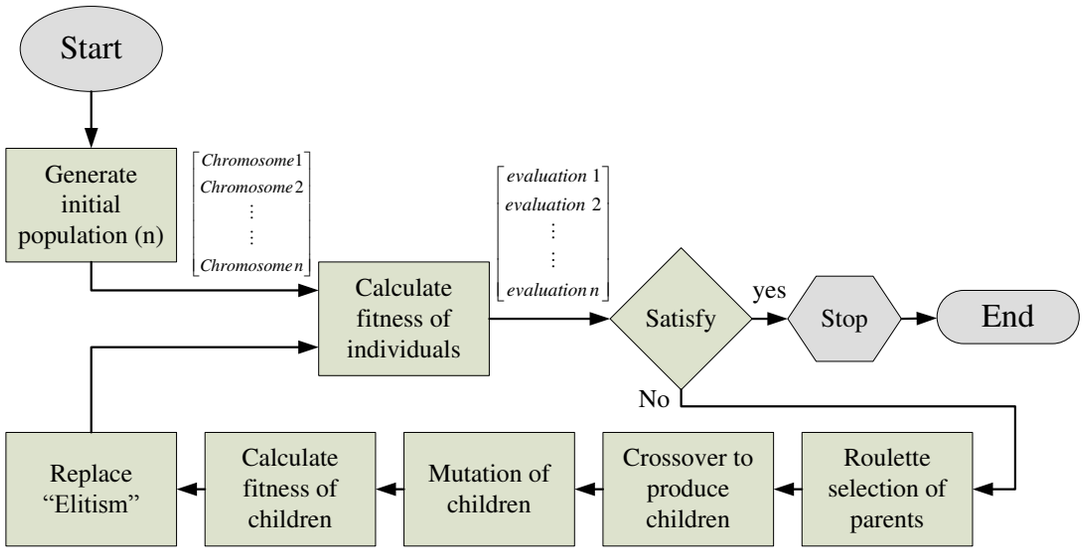

Figure 11. Flowchart procedure.

The parameters of the GA are set as below:

1. Initial population size: 30
2. Maximum number of generations: 30
3. Probability of crossover: 0.8
4. Mutation probability: 0.09
5. Performance measure: IAE

From the feedback scheme, the performance index is entertained and reverted to the genetic algorithm for the stability of the genetic process. Finally, the rule base attained is displayed as below:

$$\begin{bmatrix} 1 & 2 & 2 & 2 & 1 & 1 & 3 \\ 1 & 2 & 2 & 4 & 8 & 8 & 8 \\ 9 & 9 & 7 & 9 & 7 & 9 & 8 \end{bmatrix}$$

4. GA-optimization method

GAs are computational schemes, which on the basis of processes of natural evolution, utilize the operators who understand the process of heuristic search in a search space, in which it is presumed that the perfect solution for the optimization problem is available [22]. The process of GA is revealed in Figure 12 [21, 25].

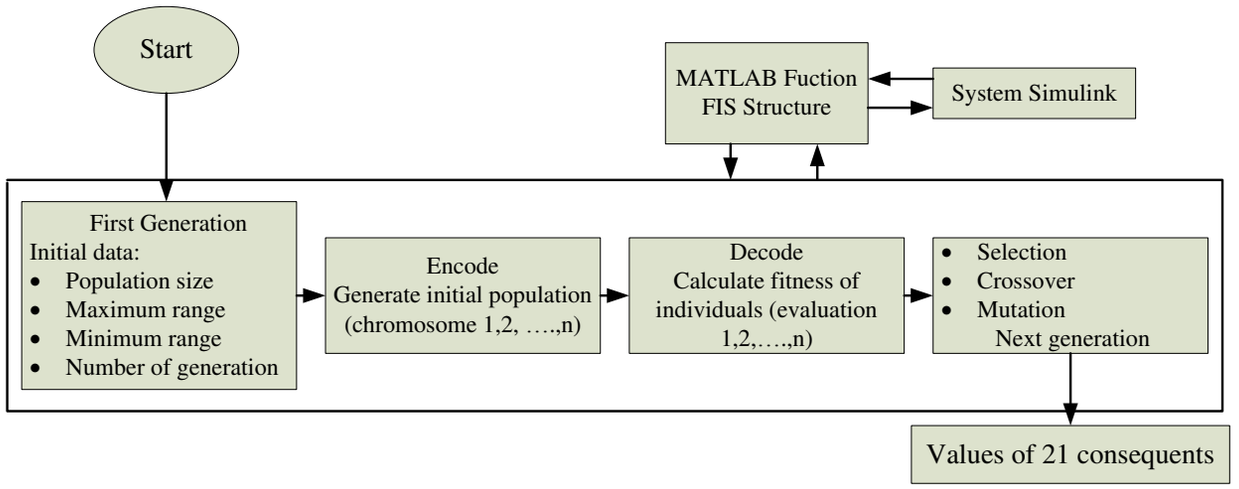

Figure 12. The process flowchart of GA.

The objective function recommended in the optimization problem is the standard *IAE* (Integrated Absolute Error) that is described by [5, 23, 26]:

$$\mathrm{IAE} = \int_0^T \left| e(t) \right| dt \tag{17}$$

The objective function recommended in Eq. (17) that is reduced in the course of the optimization process reflects a good reaction to set point changes. Among the most significant points, i.e., the decay ratio, the settling time, the rise time, the overshoot, and the steady-state error, this objective function is also considered [23]. However, merely the rule base is attained with the assistance of the optimization technique.

http://dx.doi.org/10.5772/61086

The genetic algorithm is applied to a population of individuals (chromosome) in order to devise the rules where each of them encompasses a certain fuzzy controller. The antecedents conforming to the input linguistic variables are fixed in a group as a fragment of a MATLAB function [24]. During the assessment process, this function is utilized by the genetic algorithm and it gets as arguments in the consequents of a controller; the assessment is done in all the pre-established generations for each of the individuals of the population. Also, the binary code is implemented for simplicity. The values are:

[NBB NB NM NS Z PS PM PB PBB]

And the output language variables are coded in the order:

[0001 0010 0011 0100 0101 0110 0111 1000 1001]

A likely chromosome is shown in Table 5, which would be codified as:

[0001 0010 1001 0001 0100 1001 0001 0101 1001.....1000 1001]

With the formation of a population of individuals (generated randomly), the genetic process starts in which every individual comprises the 21 consequents of a fuzzy controller in general. Since 21 consequents could be employed in the MATLAB function, to create the rules, it is essential to change the individual, codified as a binary chain, to complete numbers in the values from 1 to 9.

5. Outcomes and analysis

A combination of the fuzzy frequency controller and fuzzy current amplitude controller is used to form an HFFC. This controller provides similar supply frequency as the FOC and is insensitive to the parameter variation for the motor and system robustness to noise and load disturbances, which are the advantages of this controller. A model of HFFC for an induction motor is produced by using the MATLAB/Simulink software, which is shown in the Figure 13. Table 1 shows the parameters that are chosen to perform the simulation study.

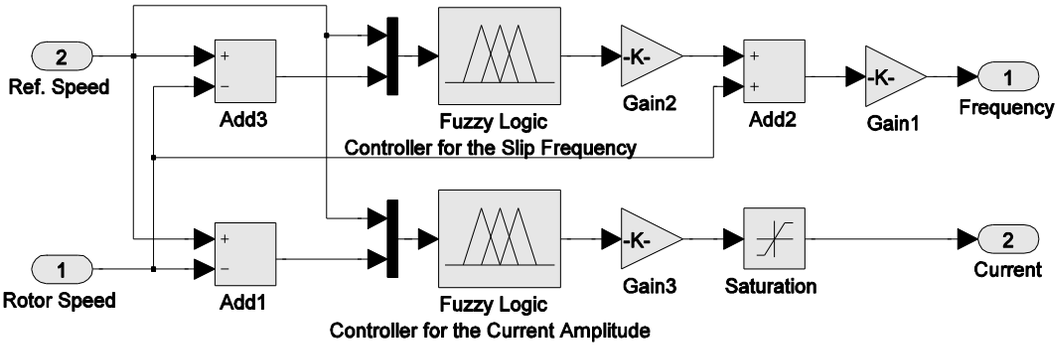

Figure 13. Simulink diagram of the HFFC.

An HFFC can be modeled by combining the fuzzy frequency controller and the fuzzy current amplitude controller. Throughout the final steady-state stage, the fuzzy frequency controller outputs the frequency that relates to the speed command. During the acceleration-deceleration stages, the fuzzy current amplitude controller outputs the maximum permitted current. The model of HFFC for the induction motor is built using MATLAB/Simulink as presented in Figure 14.

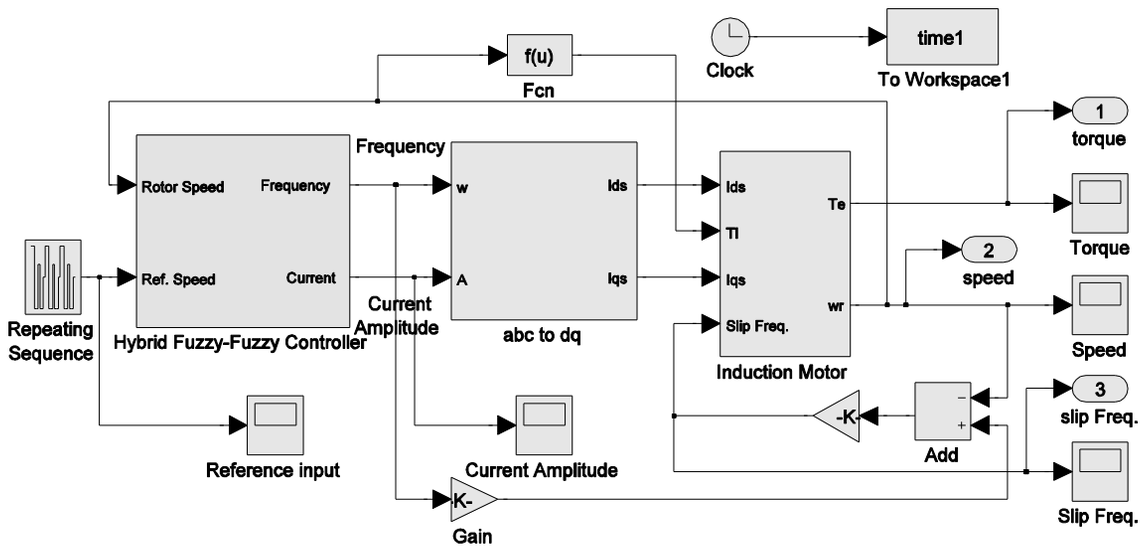

Figure 14. The model diagram of the HFFC.

6. Performance criteria

Generally, following the reference and to cast off the disturbance are the two basic key objectives of control. The following performance criterion is employed for evaluating the efficiency of the controller in achieving the aims of control for complete speed control and the performances are identified for comparisons and investigation [5, 27]. The error (e), the difference between actual and reference value, is generally categorized into a number of quantities. One of the quantities to state the accumulative error magnitude is the IAE, whose formula is given in Eq. (17) [5, 23, 26]. The quadratic measure, i.e., integral of squared error (ISE), provides the error quantitative in quadratic mode. The ISE accrues the squared error. The ISE expression is presented as:

$$\mathrm{ISE} = \int_0^T e^2(\mathrm{t})\mathrm{dt} \tag{18}$$

http://dx.doi.org/10.5772/61086

This criterion's main disadvantage is that it provides large weight if the error is large, such as, a poorly checked system. Other criteria are the integral of time weighted absolute error (ITAE) and integral of the time multiplied by the squared error (ITSE). The expression of ITAE and ITSE are articulated in Eq. (19) and Eq. (20).

$$\mathrm{ITAE} = \int_0^T t\left|e(t)\right|\mathrm{dt} \tag{19}$$

$$\mathrm{ITSE} = \int_0^T te^2(t)\mathrm{dt} \tag{20}$$

The objective of control is to reduce every performance criteria's error. The Simulink model for calculating the performance indices is presented in Figure 15 [28].

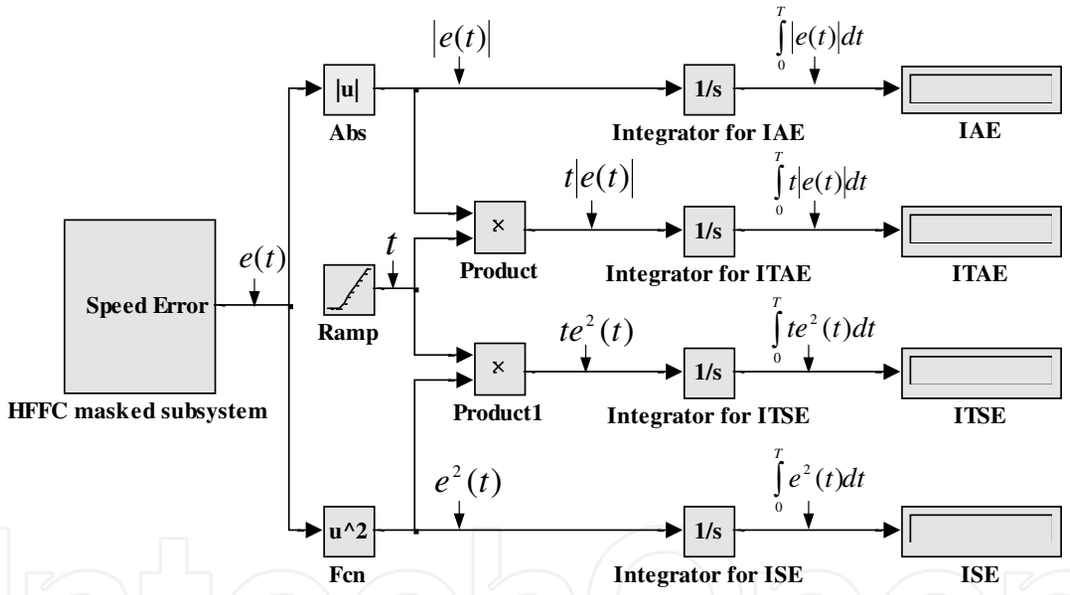

Figure 15. Simulink model for computing the performance indices.

7. Simulation results

By undertaking a simulation of an indirect rotor flux FOC, a new controller is matched with the FOC. As shown in Figure 16, the speed has augmented in 0 s from 0–120 rad/s; in 8 s period, the speed reduced to -120 rad/s; in the 12 s period, the speed has elevated to 50 rad/s; in the 16 s period, the speed has reduced to -120 rad/s; in the 18 s period, the speed has raised to 0 rad/s; and increased to 120 rad/s in the 20 s.

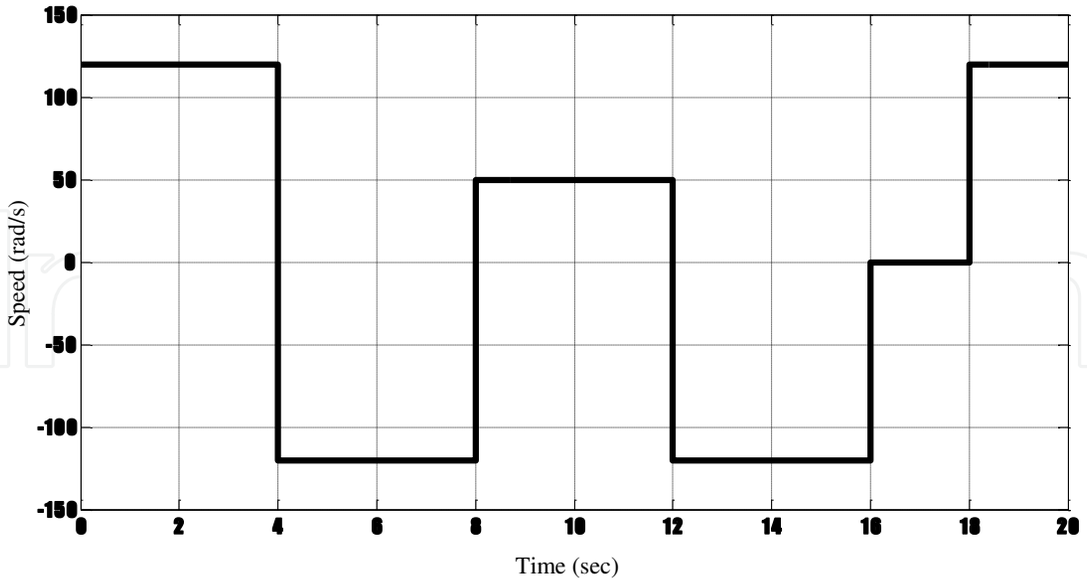

Figure 16. Reference speed step change.

The simulation outcomes of the HFFC are presented in Figures 17, 18, 19 and 20. The two-stage control method provides a very fast speed. Due to the control of the current in a final steady-state stage, the oscillations of speed are completely eliminated at a final operating point. It is evident from the comparison of these results with an IFOC with PI-controller that the HFFC shows the two features of FOC controller, i.e., the current feature at the steady state stage and the frequency feature at accelerate-decelerate stage.

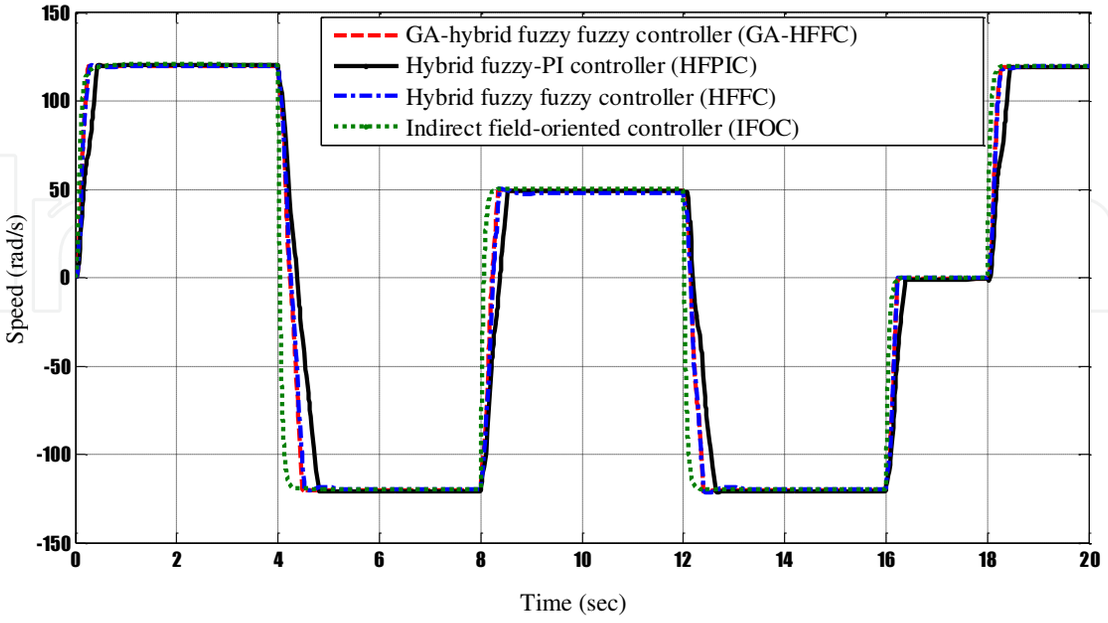

Figure 17. Fuzzy responses of the fuzzy controllers

http://dx.doi.org/10.5772/61086

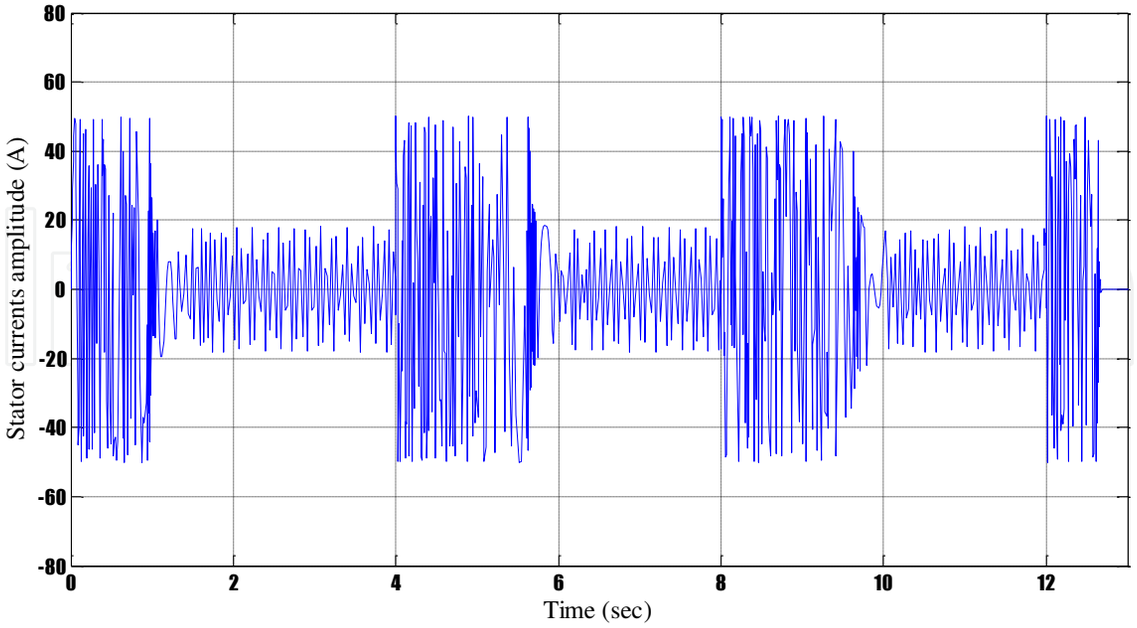

Figure 18. Stator currents amplitude of HFFC.

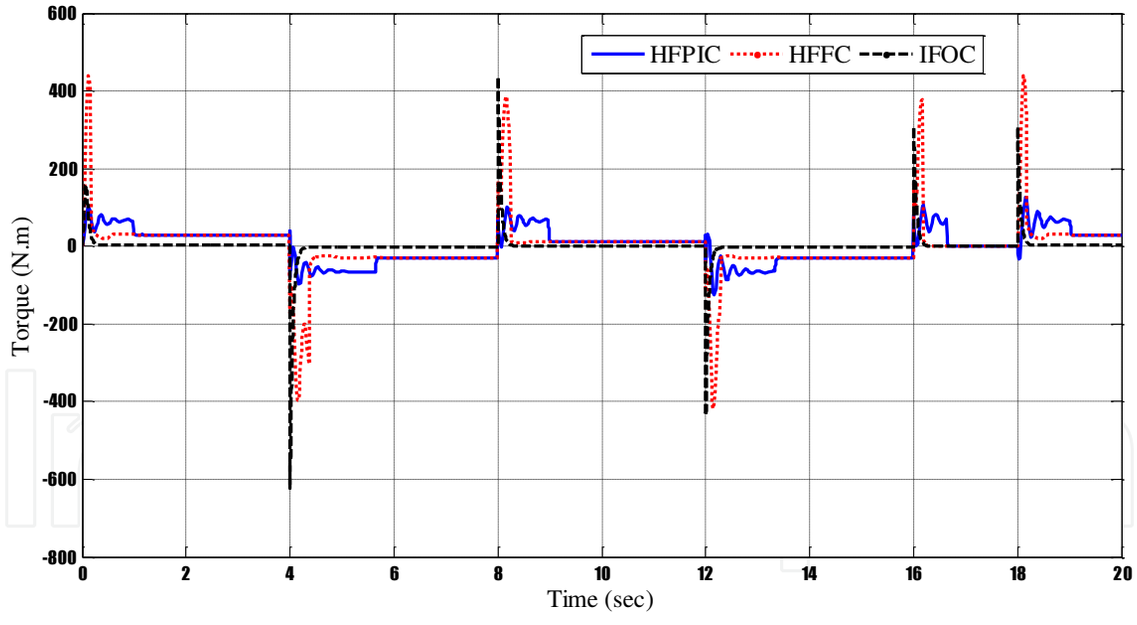

Figure 19. Torque response of HFFC.

The simulation outcomes on the efficiency of the controller centered on the performance measures are revealed in Table 7. A closer look at the overshoot, performance criteria, time rise, IAE, final steady-state value, ISE, ITAE, and ITSE is displayed to show reduced values. This validates the act of the modified controller with a better performance to effectively control the speed.

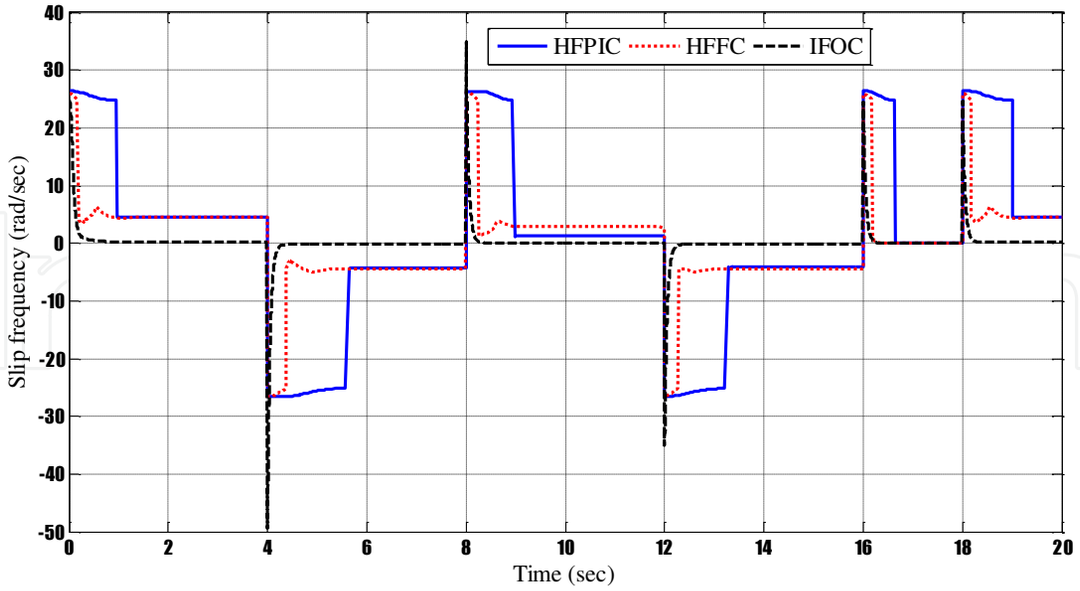

Figure 20. Slip frequency response of the fuzzy controllers.

No.	Performance Index	HFPIC	HFFC	IFOC	GA-HFFC
1	Overshoot (%)	0.000	3.000	0.000	0.000
2	Rise time (sec)	0.4363	0.2803	0.6107	0.2648
3	Final steady-state value	120.0989	120.08483	120.0681	120.08391
4	IAE	289.3	194	158.28	186
5	ISE	3.409e+004	2.311e+004	1.223e+004	2.287e+004
6	ITAE	2544	1656	1457.6	1625
7	ITSE	2.691e+005	1.765e+005	1.31e+005	1.799e+005

Table 8. The performance index comparison of the system.

8. Effects of internal and external disturbances

The mutual inductance and the rotor resistance are expected to be changed to 3 r_r and 0.8 L_M, respectively, in order to demonstrate the insensitivity of the HFFC to the variation of motor parameters. An insensitivity to the parameter variation shown by the speed response of a fuzzy controller is shown in Figure 21.

Additionally, the distributed random noises are added in the input current and the feedback speed to assess the effects of the noise of the input current and the noise of the speed sensor. The speed response to the current noise and with the measured speed illustrates that the HFFC possesses decent disturbance rejection (see Figure 22).

http://dx.doi.org/10.5772/61086

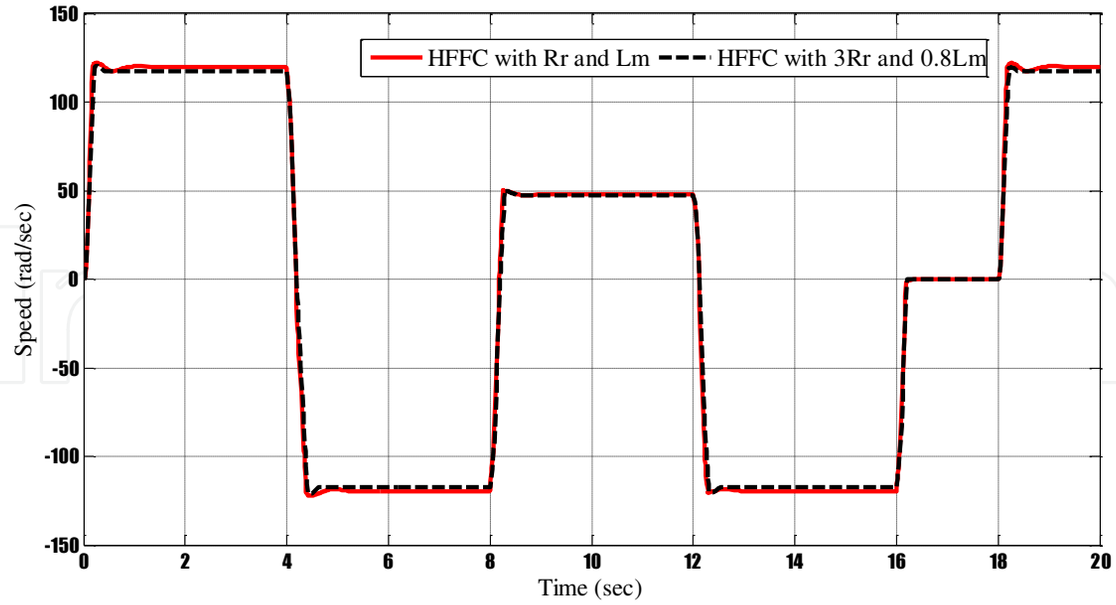

Figure 21. Speed response of HFFC with parameter variations.

Furthermore, for studying the impact of magnetic saturation of the induction motor on the controller performance, in the induction motor model, Figures 23 and 24 demonstrate the simulation results of the torque and rotor speed responses. The flux upsurge is limited, owing to the magnetic saturation so that the torque oscillations are decreased considerably, but during the acceleration-deceleration stage, an extreme magnetic saturation will create a higher temperature rise and larger losses.

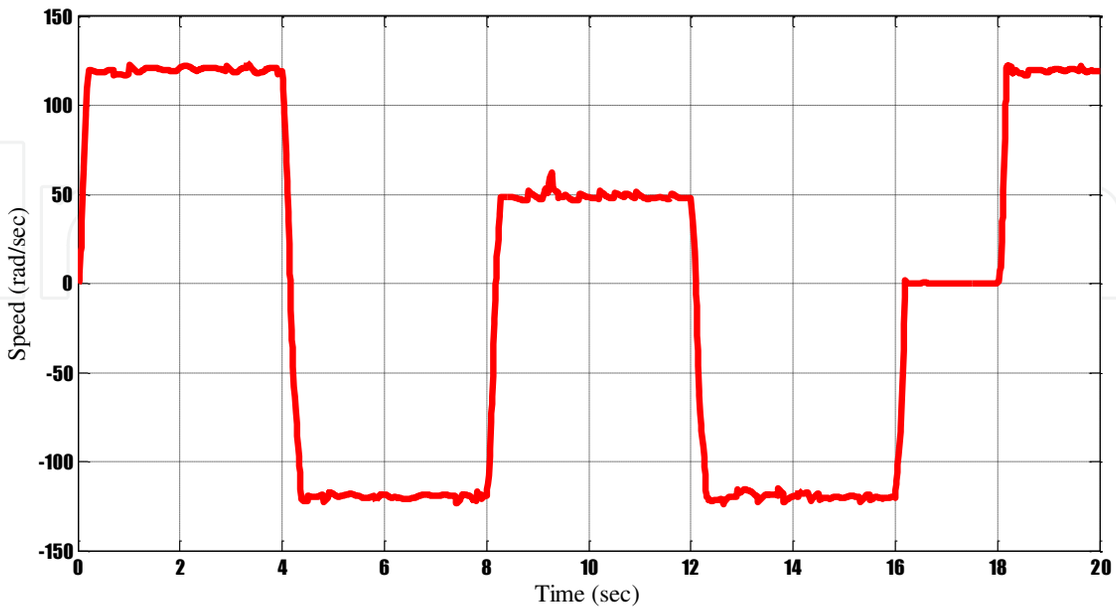

Figure 22. Speed response of HFFC with noise.

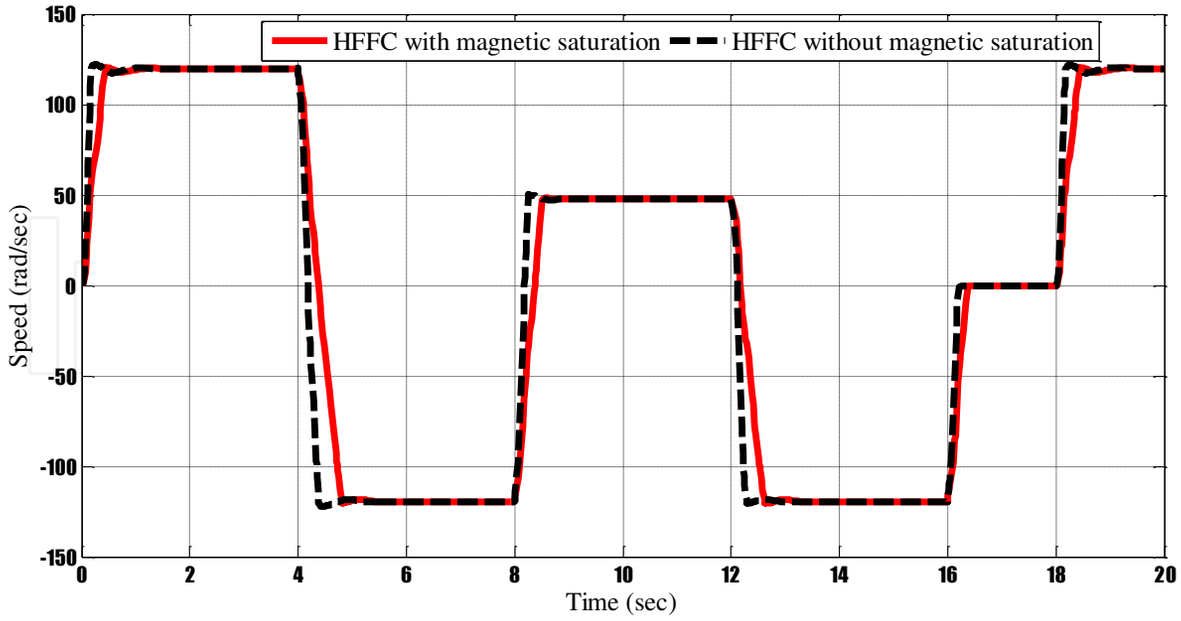

Figure 23. Speed response of HFFC with the effect of magnetic saturation.

Moreover, the effects of load torque variation on the HFFC system are analysed by the simulation. In the simulation, the control system encounters quick variations in the load torque: at t=2 s, the load increases from 0% to 100% of the rated torque, T_l, at t=7 s, the load decreases to 100% of T_l, and at t=10 s and 14 s, the load rises to 100% of T_l again, at t=19 s, the load declines to 100% of T_l.

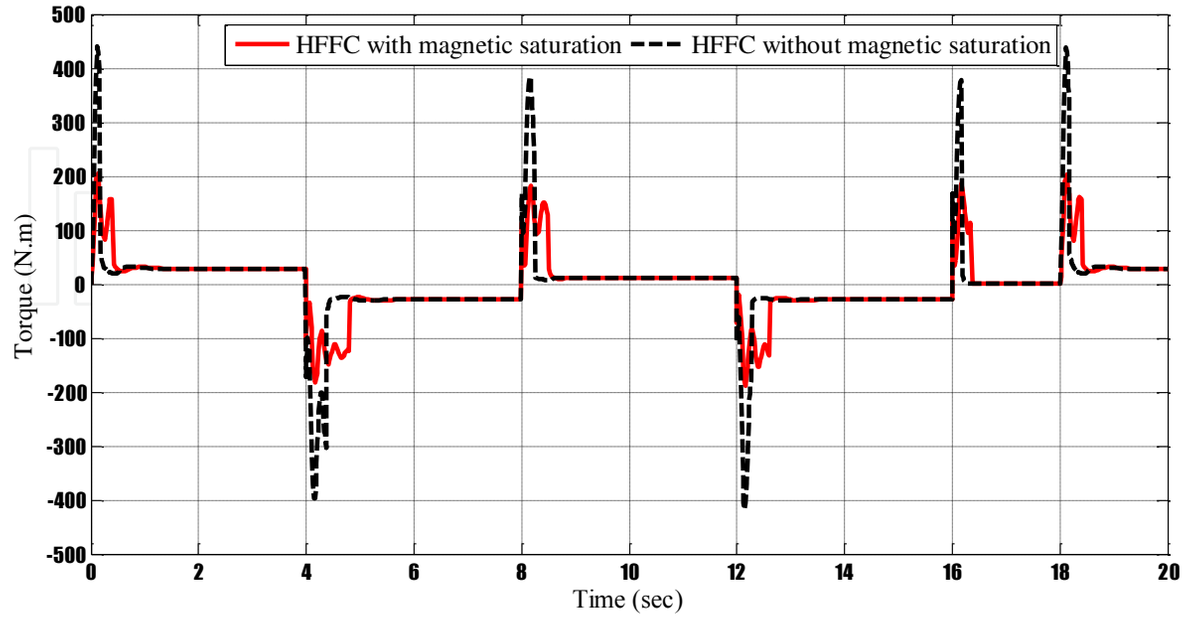

Figure 24. Torque response of HFFC with effect of magnetic saturation.

http://dx.doi.org/10.5772/61086

The torque reaction of the fuzzy-fuzzy control system with a load torque variation is demonstrated in Figure 25. The above-mentioned simulation results illustrate that the greater variations can be created in a load torque by the fuzzy-fuzzy controller. However, the extracted outcomes of performance of the model are found to be corresponding precisely with the anticipations, when it is compared with an IFOC controller. The results also reveal that the HFFC performance is unresponsive to the parameter variation for the motor and the system strength to load and noise disturbances.

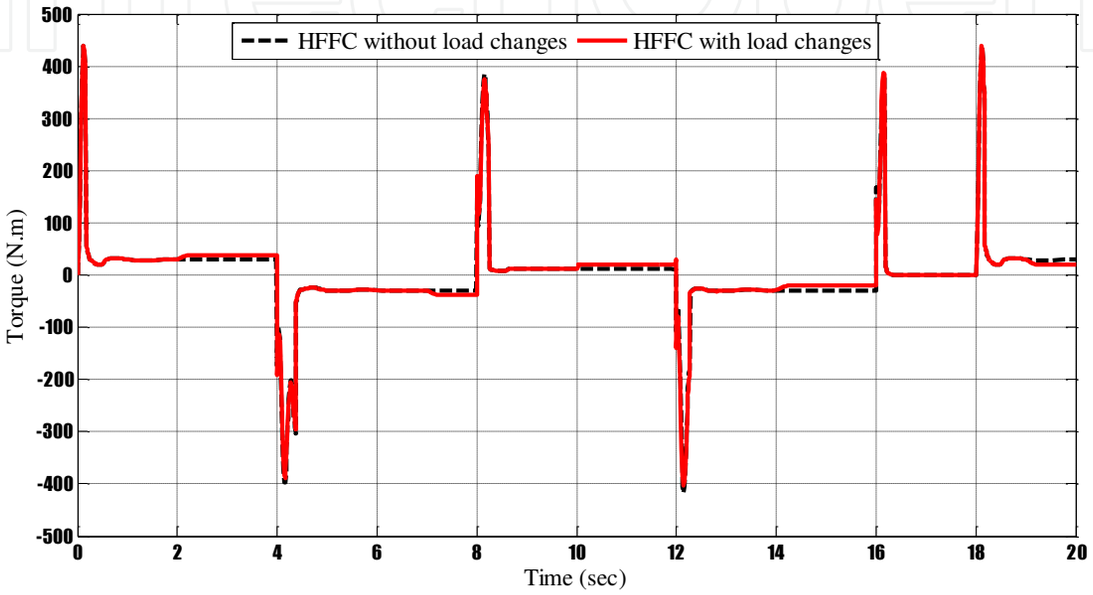

Figure 25. Torque response of HFFC with load changes.

9. The experimental results

The following experiments are conducted to demonstrate and verify the operability of the proposed controller. There are several experiments that can be conducted, however the experimental results presented here are necessary for this purpose. The experimental rig constituting the induction motor speed controller system constructed comprises of the following equipment:

- 3-phase squirrel cage induction motor 240/415 V- 175 W-1360 r/min-0.52 A-50 Hz (Lab-Volt)
- Prime Mover/Dynamometer (Lab-Volt)
- TMS320F28335 (Digital Spectrum Inc.)
- DMC1500 motor controller (Digital Spectrum Inc.)
- Tacho-generator with 500 rpm/volt
- Data acquisition card (DAQ) (Lab-Volt)

- Current sensors
- LVDAM-EMS software for DAQ
- Host PC

Figure 26 (a), (b), and (c) demonstrate the three-phase voltages waveforms $V_{a,}$ V_b, and V_c, respectively, acquired by DAQ. The actual voltages are 120° different phases from each other.

Figures 27 (a), (b), and (c) show the three-phase sinusoidal PWM for an inverter-fed induction motor in a TMS320F28335 eZdsp control card. These signals are the output from the digital signal processor (DSP) that have been applied to the inverter to control the induction motor. The frequency of switching has been set at 10 kHz. It is worth to point out that for this controller the operating frequency can be applied between 0 to 10 kHz.

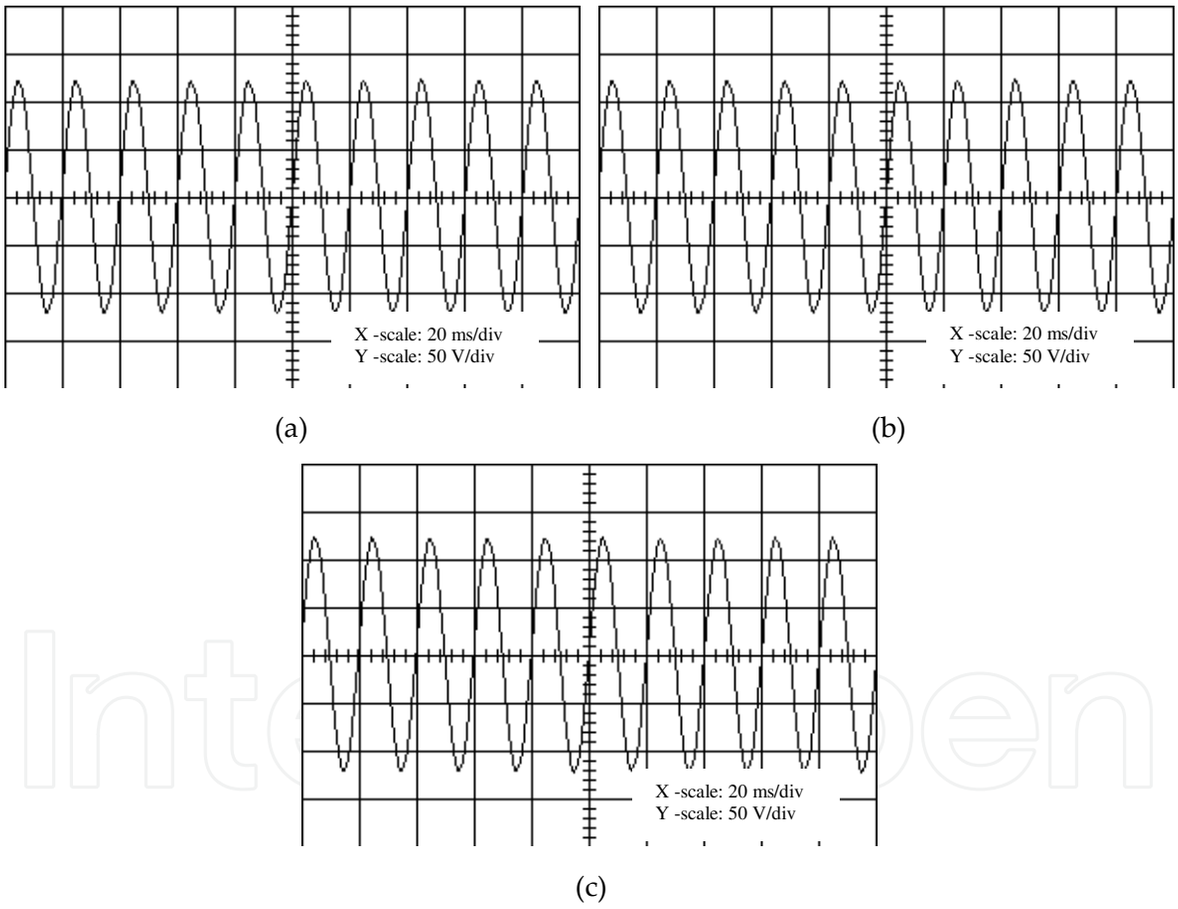

Figure 26. (a) V_a , (b) V_b and (c) V_c waveforms output.

In Figure 28 (a) and (b) are the output signals measured by the encoder at two different sampling rates: 5 kHz and 10 kHz, respectively, which demonstrate the different speeds that can be achieved. The encoder is providing signal to the controller that represents the feedback signals.

http://dx.doi.org/10.5772/61086

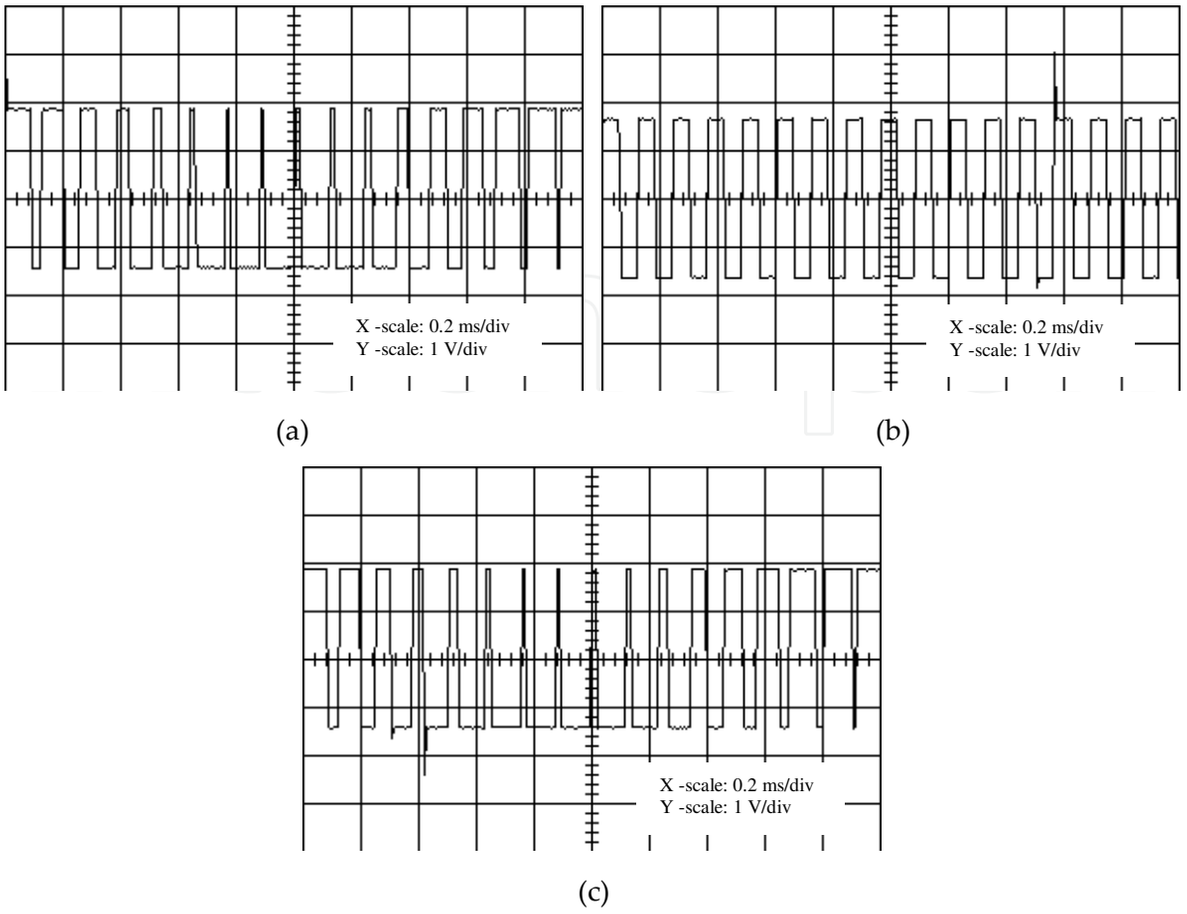

Figure 27. The three-phase PWM. (a) PWM1, (b) PWM2, and (c) PWM3.

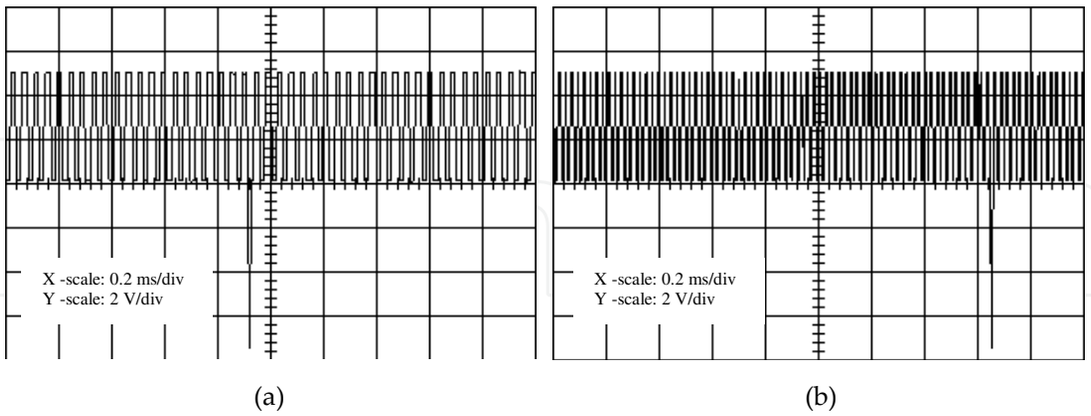

Figure 28. Encoder output signals at different sampling rate (a) 5 kHz and (b) 10 kHz.

Figure 29 (a), (b), and (c) show the stator voltage and current in the acceleration and steady-state stages and speed response in the steady-state stage, respectively, looking at one of the three phases. Figure 29 (a) reveals the stator voltage that increases gradually to a constant value. For the stator current, as shown in Figure 29 (b), the current is initially at maximum

value and gradually decreases to a constant value. These verify that the controller is performing as expected during the acceleration and steady-state stages. Figure 29 (c) represents the speed at steady-state stage, which also proves that the controller is performing as expected, though some spikes are observed that can be related to the encoder used in this set-up. The spikes can be eliminated if a more sensitive encoder has been used.

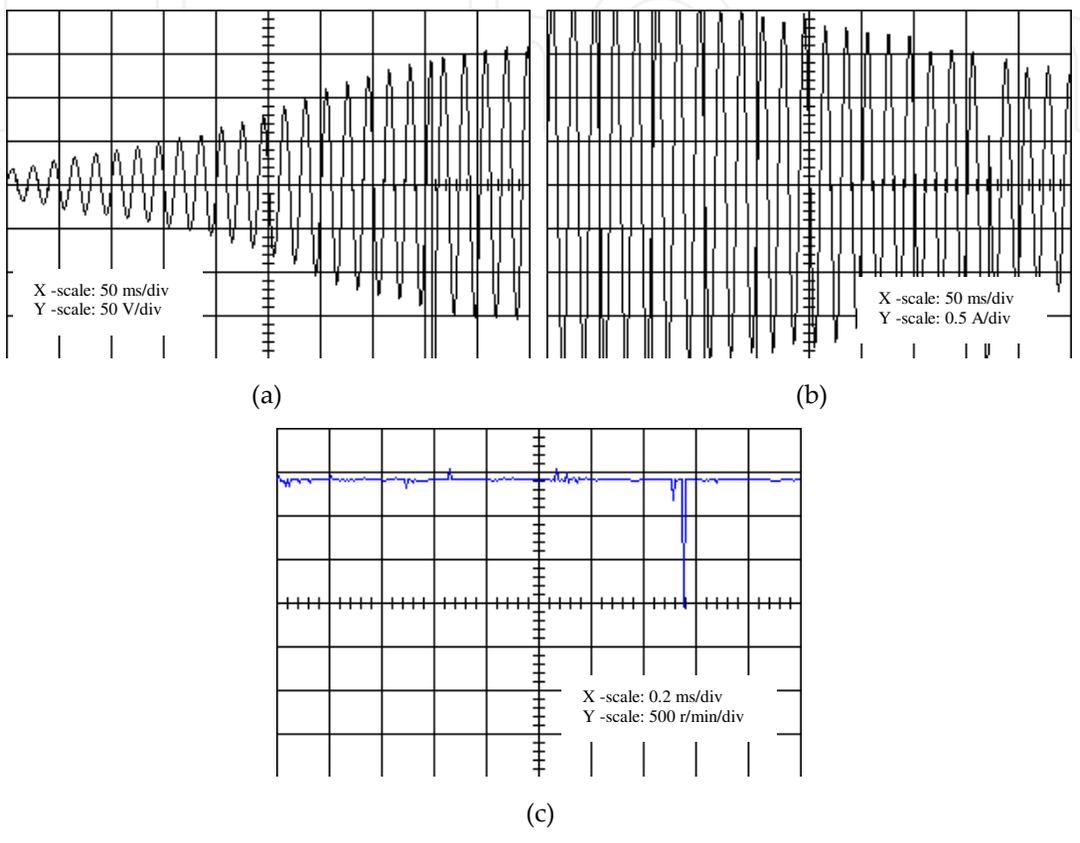

Figure 29. (a) Stator voltage, (b) stator current, and (c) speed response outputs.

10. Conclusions

The objective of this study is to elaborate and elucidate the effects and performance of internal and external disturbances for an established HFFC scheme to accordingly modify the speed of an induction motor. The fuzzy-fuzzy controller has been proven to be more effective as compared to a scalar controller due to the utilisation of the two aspects of the FOC. Besides, one of the key advantages of this controller includes the supply of the same FOC and frequency that is unresponsive to the parameter variation in the motor and system strength to noise and load disturbances. This study, under dynamic settings, produced a comprehensive evaluation and analysis of the three controllers, HFFC, IFOC, and HFPIC. The experimental results verify the performance of the proposed HFFC in controlling the IM variable speed drive. Therefore,

for further enhancing the IM-VSD performance, the work to be considered includes the advancement in the augmentation of the controllers to improve the VSD performances.

Acknowledgements

The authors acknowledge the support from the Universiti Teknologi PETRONAS through the award of the Graduate Assistantship scheme and URIF.

Author details

Nordin Saad*, Muawia A. Magzoub, Rosdiazli Ibrahim and Muhammad Irfan

*Address all correspondence to: nordiss@petronas.com.my

Department of Electrical and Electronic Engineering, Universiti Teknologi Petronas, Bandar Sri Iskandar, Perak, Malaysia

References

[1] J. Bocker and S. Mathapati. State of the art of induction motor control. In: IEEE International Electric Machines & Drives Conference; May; 2007. p. 1459-1464.

[2] Muawia Magzoub, Nordin Saad, and Rosdiazli Ibrahim. Analysis and modeling of indirect field-oriented control for PWM-driven induction motor drives. In: 2013 IEEE Conference on Clean Energy and Technology (CEAT); November; IEEE; 2013. p. 488-493.

[3] M. Magzoub, N. Saad, and R. Ibrahim. An intelligent speed controller for indirect field-oriented controlled induction motor drives. In: 2013 IEEE conference on Clean Energy and Technology (CEAT); November; IEEE; 2013. p. 327-331.

[4] M. Magzoub, N. Saad, R. Ibrahim, M. Maharun, and S. Zulkifli. Hybrid fuzzy-fuzzy controller for PWM-driven induction motor drive. In: 2014 IEEE International Conference on Power and Energy (PEcon); IEEE; 2014. p. 260-265.

[5] N. Saad and M. Arrofiq. A PLC-based modified-fuzzy controller for PWM-driven induction motor drive with constant V/Hz ratio control. Robotics and Computer-Integrated Manufacturing. 2012;28(2):95-112.

[6] K. L. Shi, T. F. Chan, and Y. K. Wong. Hybrid fuzzy two-stage controller for an induction motor. In: 1998 IEEE International Conference on Systems, Man, and Cybernetics; October; IEEE; 1998. p. 1898-1903.

[7] K. L. Shi, T. F. Chan, Y. K. Wong, and S. L. Ho. An improved two-stage control scheme for an induction motor. In: Proceedings of the IEEE 1999 International Conference on Power Electronics and Drive Systems; IEEE; 1999. p. 405-410.

[8] K. L. Shi, T. F. Chan, Y. K. Wong, and S. L. Ho. A novel hybrid fuzzy/PI two-stage controller for an induction motor drive. In: IEMDC 2001. IEEE International Electric Machines and Drives Conference; IEEE; 2001. p. 415-421.

[9] D. Asija. Speed control of induction motor using fuzzy-PI controller. In: 2010 2nd International Conference on Mechanical and Electronics Engineering (ICMEE); August; IEEE; 2010. p. V2-460.

[10] N. Tiwary, A. Rathinam, and S. Ajitha. Design of hybrid fuzzy-pi controller for speed control of brushless dc motor. In: 2014 International Conference on Electronics, Communication and Instrumentation (ICECI); January; IEEE; 2014. p. 1-4.

[11] P. Melin and O. Castillo, editors. Hybrid intelligent systems for pattern recognition using soft computing: an evolutionary approach for neural networks and fuzzy systems. Springer Science & Business Media; 2005.

[12] W. S. Oh, Y. T. Kim, C. S. Kim, T. S. Kwon, and H. J. Kim. Speed control of induction motor using genetic algorithm based fuzzy controller. In: The 25th Annual Conference of the IEEE, In Industrial Electronics Society; IEEE; 1999. p. 625-629.

[13] S. V. Wong and A. M. S. Hamouda. Optimization of fuzzy rules design using genetic algorithm. Advances in Engineering Software. 200;31(4):251-262.

[14] I. K. Bousserhane, A. Hazzab, M. Rahli, M. Kamli, and B. Mazari. Adaptive PI controller using fuzzy system optimized by genetic algorithm for induction motor control. In: 10th IEEE, In International Power Electronics Congress; IEEE; 2006. p. 1-8.

[15] J. Y. Zhang and Y. D. Li. Application of genetic algorithm in optimization of fuzzy control rules. In: Proceedings of the Sixth International Conference on Intelligent Systems Design and Applications; IEEE Computer Society; 2006.

[16] H. X. Zhang, B. Zhang, and F. Wang. Automatic fuzzy rules generation using fuzzy genetic algorithm. In: 2009 Sixth International Conference on Fuzzy Systems and Knowledge Discovery; IEEE; 2009. p. 107-112.

[17] M. A. Jaradat, M. I. Awad, and B. S. El-Khasawneh. Genetic-fuzzy sliding mode controller for a dc servomotor system. In: 2012 8th International Symposium on Mechatronics and its Applications (ISMA); IEEE; 2012. p. 1-6.

[18] A. Trzynadlowski. The field orientation principle in control of induction motors. Springer Science & Business Media; 1993.

[19] K. Bimal. Bose. Modern power electronics and AC drives. 2002.

[20] M. Magzoub, N. Saad, and R. Ibrahim. Simulation of a ball on a beam model using a fuzzy-dynamic and a fuzzy-static sliding-mode controller. Research Journal of Applied Sciences, Engineering and Technology. 2014;8(2):288-295.

[21] T. F. Chan and K. Shi. Applied intelligent control of induction motor drives. John Wiley & Sons; 2011. 421 p.

[22] N. Siddique, editor. Intelligent control a hybrid approach based on fuzzy logic, neural networks and genetic algorithms. Springer International Publishing Switzerland 2014; 2014. 282 p. DOI: 10.1007/978-3-319-02135-5

[23] N. Pitalúa Díaz, R. Lagunas Jiménez, and A. González. Tuning fuzzy control rules via genetic algorithms: An experimental evaluation. Research Journal of Recent Sciences. 2013;2(10):81-87.

[24] J. S. R. Jang and and N. Gulley, editors. Fuzzy logic toolbox user's guide. Second printing ed. The MathWorks, Inc.; April 1997. p. 208.

[25] Genetic algorithm and direct search toolbox user's guide. The MathWorks, Inc.; January 2004. p. 210.

[26] M. Nuruzzaman, editor. Modeling and simulation in SIMULINK for engineers and scientists. AuthorHouse; 2005.

[27] O. Wahyunggoro and N. Saad. Development of fuzzy-logic-based self-tuning PI controller for servomotor. In: S. Ehsan Shafiei, editor. Advanced Strategies for Robot Manipulators. Sciyo; August, 2010.

[28] S. Lynch, editor. Dynamical systems with applications using MATLAB. Springer International Publishing; 2014. p. 519.

IntechOpen